Neutral donors and spin-flip Raman spectra in dilute-magnetic-semiconductor microstructures

W. E. Hagston, P. Harrison, and T. Stirner
Department of Applied Physics, University of Hull, Kingston upon Hull HU6 7RX, Great Britain
(Received 20 October 1993)

An approach is presented for calculating the binding energy of neutral donors in semiconductor heterostructures. The technique avoids the need for analytical solutions. A generalization of the method to include central cell corrections, effective mass, and dielectric mismatch at heterojunctions, together with band nonparabolicity, is discussed. The utility of the method is demonstrated via a study of the spin-flip Raman spectrum of double quantum wells. Finally it is shown how spin-flip Raman spectroscopy could be used, in conjunction with δ doping of donors, as a probe of the possible enhancements to the paramagnetism of a dilute magnetic semiconductor at a heterojunction with a nonmagnetic material.

I. INTRODUCTION

Theoretical treatments of donors in quantum well systems have centered around two basic methods. The first involves expanding the electron wave function as a linear combination of Gaussian functions.[1,2] While this technique has been successful in calculating the properties of donors in simple quantum well structures, generalization to more complex structures, including graded gap materials and systems where piezoelectric fields are present, is nontrivial.

Another approach chooses a trial wave function as a product of two terms, i.e.,

$$\Psi = \psi(z)e^{-\frac{r'}{\lambda}}, \tag{1}$$

where r' is the electron-donor separation, λ is a variational parameter, and $\psi(z)$ is the uncorrelated eigenfunction of the electron in the quantum well *without* the donor.[3,4] The purpose of the present work is to show that the latter restriction can be removed and that a more general choice of the donor wave function Ψ can be made. Furthermore the formalism developed can be applied to a donor in *any* semiconductor quantum well (micro)structure, independently of whether analytical one-particle solutions for $\psi(z)$ exist.[5]

The paper describes the inclusion of central cell corrections and demonstrates how band nonparabolicity and dielectric and effective mass mismatch can be included in the theory. In order to illustrate the utility of the formalism, a study of spin-flip Raman spectroscopy in dilute magnetic semiconductor double quantum wells is presented. Furthermore it is shown how this experimental technique could be used to investigate the magnetic properties of heterointerfaces between magnetic and nonmagnetic semiconductors.

II. THEORY

Any theoretical study of the properties of neutral donors in semiconductor quantum well structures necessitates solving the standard Schrödinger equation[6] for such structures but with the inclusion of the additional Coulombic term representing the donor potential. With a view to generality, the aim of the following is to recast this problem in a form which is suitable for numerical solution thus making it applicable to any quantum well structure, be it a double quantum well, a diffused quantum well, or a graded gap quantum well, etc.

A. Binding energy of a neutral donor in a semiconductor heterostructure

Without loss of generality we choose our coordinate system so that the Hamiltonian of an electron confined in a semiconductor heterostructure defined by the one-dimensional potential $\mathcal{V}(z)$ is given by

$$\mathcal{H} = -\frac{\hbar^2}{2m^*}\nabla^2 + \mathcal{V}(z) - \frac{e^2}{4\pi\epsilon r'}, \tag{2}$$

where

$$r'^2 = x^2 + y^2 + (z - r_d)^2 = x^2 + y^2 + z'^2 \tag{3}$$

and r_d is the position of the donor along the growth (z) direction. The z dependence of the wave function Ψ of an electron in such a system is taken to have the form

$$\Psi = \chi(z)e^{-\frac{r'}{\lambda}}, \tag{4}$$

where the one-dimensional envelope function $\chi(z)$ is yet to be determined. The isotropy of the hydrogenic-type factor $e^{-\frac{r'}{\lambda}}$, i.e., the fact that the x-y coordinates are assigned the same variational parameter $1/\lambda$ as the z coordinate, was implied by detailed calculations we have carried out on excitons in quantum wells.[7] The Schrödinger equation corresponding to the Hamiltonian of Eq. (2) contains a term of the form $\nabla^2\Psi$ which can be shown to be given by

$$\nabla^2\Psi = [\nabla_z^2\chi(z)]e^{-\frac{r'}{\lambda}} + 2\nabla_z\chi(z)\nabla_z e^{-\frac{r'}{\lambda}} + \chi(z)\nabla^2 e^{-\frac{r'}{\lambda}}. \tag{5}$$

Hence the Schrödinger equation becomes

$$-\frac{\hbar^2}{2m^*}\left\{[\nabla_z^2\chi(z)]e^{-\frac{r'}{\lambda}}+2\nabla_z\chi(z)\nabla_z e^{-\frac{r'}{\lambda}}+\chi(z)\nabla^2 e^{-\frac{r'}{\lambda}}\right\}$$

$$-\frac{e^2}{4\pi\epsilon r'}\chi(z)e^{-\frac{r'}{\lambda}}+\mathcal{V}(z)\chi(z)e^{-\frac{r'}{\lambda}}=E\chi(z)e^{-\frac{r'}{\lambda}}, \quad (6)$$

where E is the total energy of the electron in the donor–quantum-well system. Multiplying by $e^{-\frac{r'}{\lambda}}$ and integrating over the xy plane leads to an equation of the form

$$-\frac{\hbar^2}{2m^*}\left[\nabla_z^2\chi(z)I_1+2\nabla_z\chi(z)I_2+\chi(z)I_3\right]$$

$$-\frac{e^2}{4\pi\epsilon}\chi(z)I_4+\mathcal{V}(z)\chi(z)I_1=E\chi(z)I_1, \quad (7)$$

where the integrals $I_j, j=1,2,3,4$ are defined below:

$$I_1=\int_0^\infty\int_0^\infty e^{-\frac{2r'}{\lambda}}\,dx\,dy=\int_0^\infty e^{-\frac{2r'}{\lambda}}\,2\pi\,r_\perp\,dr_\perp, \quad (8)$$

where $r_\perp^2=x^2+y^2$. Now

$$r'^2=r_\perp^2+z'^2. \quad (9)$$

Therefore $r'dr'=r_\perp dr_\perp$; hence

$$I_1=\int_{|z'|}^\infty e^{-\frac{2r'}{\lambda}}\,2\pi\,r'\,dr', \quad (10)$$

which can be integrated by parts to give

$$I_1=2\pi\left(\frac{\lambda|z'|}{2}+\frac{\lambda^2}{4}\right)e^{-\frac{2|z'|}{\lambda}}. \quad (11)$$

Also

$$I_2=\int_0^\infty\int_0^\infty e^{-\frac{r'}{\lambda}}\nabla_z e^{-\frac{r'}{\lambda}}\,dx\,dy \quad (12)$$

can be evaluated by parts to give

$$I_2=2\pi\left(-\frac{z'}{2}\right)e^{-\frac{2|z'|}{\lambda}}. \quad (13)$$

The third integral

$$I_3=\int_0^\infty\int_0^\infty e^{-\frac{r'}{\lambda}}\nabla^2 e^{-\frac{r'}{\lambda}}\,dx\,dy \quad (14)$$

can be transformed, as in the Appendix, and integrated by parts to give

$$I_3=2\pi\left(\frac{|z'|}{2\lambda}-\frac{3}{4}\right)e^{-\frac{2|z'|}{\lambda}} \quad (15)$$

and finally

$$I_4=\int_0^\infty\int_0^\infty\frac{e^{-\frac{2r'}{\lambda}}}{r'}\,dx\,dy=2\pi\left(\frac{\lambda}{2}\right)e^{-\frac{2|z'|}{\lambda}}. \quad (16)$$

Substituting the integrals I_1, I_2, I_3, and I_4 into Eq. (6) gives after some manipulation

$$-\frac{1}{2}\frac{\partial^2\chi}{\partial z^2}+\frac{z'}{\lambda(|z'|+\lambda/2)}\frac{\partial\chi}{\partial z}+\left[-\frac{1}{2\lambda^2}+\frac{1}{\lambda(|z'|+\lambda/2)}\right.$$

$$\left.-\frac{e^2m^*}{4\pi\epsilon\hbar^2}\frac{1}{(|z'|+\lambda/2)}+\frac{\mathcal{V}(z)m^*}{\hbar^2}-\frac{Em^*}{\hbar^2}\right]\chi=0, \quad (17)$$

which can be solved numerically[8,9] for any value of the parameter λ, according to the boundary conditions of exponential decay of the envelope function $\chi(z)$ into the outer barriers of the heterostructure as $z\longrightarrow\pm\infty$. The parameter λ was varied to minimize the total energy E of the electron.

An important point to note is that no assumptions about the form of $\mathcal{V}(z)$ have been made in the above derivation. Hence the formalism can be applied to *any* heterostructure simply by employing the appropriate form of the potential $\mathcal{V}(z)$.

B. Inclusion of a central cell correction

The central cell correction allows for a change in the permittivity of the material as the electron approaches the donor, i.e., the degree of electronic shielding is reduced and the permittivity changes. As a consequence the Coulombic potential term contains an additional factor, which, for the purpose of illustration, is taken to be as follows:

$$-\frac{e^2}{4\pi\epsilon r'}\longrightarrow-\frac{e^2}{4\pi\epsilon r'}\left(1+\Xi e^{-\frac{r'}{\Lambda}}\right), \quad (18)$$

where Λ is a parameter describing the extent of the correction. As $r'\longrightarrow 0$ it is expected that

$$-\frac{e^2}{4\pi\epsilon r'}\left(1+\Xi e^{-\frac{r'}{\Lambda}}\right)\longrightarrow-\frac{e^2}{4\pi\epsilon_0 r'}, \quad (19)$$

where ϵ_0 is the permittivity of free space. Taking this limit gives

$$\frac{1}{\epsilon}(1+\Xi)=\frac{1}{\epsilon_0}, \quad (20)$$

i.e.,

$$\Xi=\frac{\epsilon}{\epsilon_0}-1. \quad (21)$$

The effect of these changes on the single donor analysis carried out above occurs solely in the integral I_4 which becomes

$$I_4'=\int_0^\infty\int_0^\infty\left(1+\Xi e^{-\frac{r'}{\Lambda}}\right)\frac{e^{-\frac{2r'}{\lambda}}}{r'}\,dx\,dy. \quad (22)$$

This then gives

$$I_4'=I_4+2\pi\Xi\frac{\Lambda\lambda}{\lambda+2\Lambda}e^{-\frac{|z'|}{\Lambda}}e^{-\frac{|z'|}{\lambda}}. \quad (23)$$

Hence the addition of such a central cell correction leads to an additional term in Eq. (7), with the corresponding form of Eq. (17) being

$$-\frac{1}{2}\frac{\partial^2\chi}{\partial z^2}+\frac{z'}{\lambda(|z'|+\lambda/2)}\frac{\partial\chi}{\partial z}+\left[-\frac{1}{2\lambda^2}+\frac{1}{\lambda(|z'|+\lambda/2)}\right.$$

$$-\frac{e^2m^*}{4\pi\epsilon\hbar^2}\frac{1}{(|z'|+\lambda/2)}\left(1+\frac{2\Xi\Lambda}{\lambda+2\Lambda}e^{-\frac{|z'|}{\Lambda}}\right)$$

$$\left.+\frac{\mathcal{V}(z)m^*}{\hbar^2}-\frac{Em^*}{\hbar^2}\right]\chi=0. \quad (24)$$

C. Effective mass and dielectric mismatch at the heterojunction

A great deal of attention has been paid in the literature to the role of effective mass mismatch at interfaces in semiconductor heterostructures, e.g., Bastard,[6] and to the effect this may have on donor energies. In particular Fraizzoli *et al.*[10] have studied in detail the role of a dielectric constant mismatch at interfaces between dissimilar materials and its effect on shallow donor impurity levels in GaAs-$Ga_{1-x}Al_xAs$ quantum well structures. Such considerations can be readily incorporated in the present approach and from a formal point of view simply involve making allowance for the fact that

$$m^* \longrightarrow m^*(z), \quad \epsilon \longrightarrow \epsilon(z), \quad (25)$$

i.e., these two parameters have a z dependence.

In the material system considered later, i.e., CdTe-$Cd_{1-x}Mn_xTe$ with low x, in view of the lack of experimental evidence to the contrary, both of these dependencies are neglected. However, as noted earlier, their inclusion in the theory is straightforward and in certain systems, e.g., $Ga_{1-x}Al_xAs$, is deemed necessary.[1]

D. Band nonparabolicity

Small well widths and large potential barriers could require the inclusion of the nonparabolicity of the conduction band.[3] Ekenberg[11] described the inclusion of nonparabolicity on the subband structure of quantum wells. This method can account accurately for a variety of physical phenomena, but is analytically complicated. Simpler procedures have been proposed by various authors for the more complex problem of a donor in a quantum well. For example, Chaudhuri and Bajaj[3] used the simple replacement

$$m^* \longrightarrow m^*(E) = a_0 + a_1E + a_2E^2 + a_3E^3 + \cdots + a_nE^n, \quad (26)$$

where the a_n are a series of constants. Given the values of these constants, the effects of nonparabolicity can be readily incorporated into Eq. (17) since the energy E is simply a parameter that is evaluated numerically. However, one must always bear in mind the limitations of such approximations.

In relation to the calculations below, we note that Chaudhuri and Bajaj[3] showed that, even with relatively large potential barriers, band nonparabolicity was only significant for wells narrower than half the Bohr radius of the neutral donor. In the $Cd_{1-x}Mn_xTe$ system of interest here, the Bohr radius λ is typically 70 Å; hence even if the potential barriers were of comparable height to those in $Ga_{1-x}Al_xAs$, band nonparabolicity would only be significant for wells of width < 35 Å. Since the barrier heights are significantly smaller in the CdTe-$Cd_{1-x}Mn_xTe$ system than in the GaAs-$Ga_{1-x}Al_xAs$ system (typically <100 meV in the conduction band for a barrier manganese concentration x <0.1), band nonparabolicity effects are expected to be small. For this reason they are neglected in the present work, since their inclusion will only have a minor effect on the essential points that are made later.

III. RESULTS AND DISCUSSION

A. Comparison of trial wave functions

We illustrate first the difference between the exact numerical result for the one-dimensional function $\chi(z)$, as given by the solution of Eq. (17), and the one-electron wave function $\psi(z)$ appropriate to the Hamiltonian of Eq. (2) but neglecting the donor potential (i.e., the third term on the right-hand side). Consider Fig. 1, which compares the envelope functions $\psi(z)$ and $\chi(z)$ of an electron in a 100 Å CdTe well surrounded by 200 Å barriers of $Cd_{1-x}Mn_xTe$, with x=0.075. The donor is situated at the well-barrier interface, i.e., it is located at z=200 Å, since the origin of the coordinates is placed at the left-hand edge of the structure. (In all calculations 60% of the total band discontinuity between the well and barrier materials was taken to lie in the conduction band, in agreement with recent work.[12]) Note that, although the envelope function $\chi(z)$ appears to have moved to the right, and therefore away from the donor, when the hydrogen-

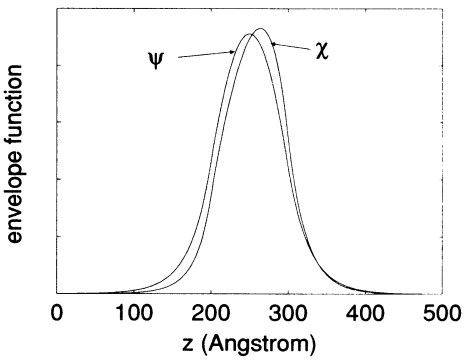

FIG. 1. Comparison of the envelope functions χ and Ψ for an electron bound to a donor situated at the well-barrier interface (r_d=200 Å) of a 100 Å quantum well.

like factor $e^{-\frac{r'}{\lambda}}$ is included, the complete wave function Ψ, as given by Eq. (4), is indeed localized towards the donor. It is clearly demonstrated that, although $\psi(z)$ may be considered to be a good choice of wave function, it is merely an approximation and does differ significantly from the one-dimensional solution $\chi(z)$. The difference between the two functions is reduced as the donor moves further into the barrier where it has less influence on the electron. The similarity between the two wave functions is also increased when the donor is located at the center of the well and hence preserves the symmetry appropriate to $\psi(z)$. However, even in the latter case, $\chi(z)$ is slightly more localized within the well than $\psi(z)$, which is to be expected given the attractive nature of the Coulomb potential.

B. Effect of central cell correction

Figure 2 shows the effect of varying the central cell parameter Λ on the total electron energy E, for donors located either at the center of the 100 Å well described above (i.e., r_d is given by z=250 Å) or at the first well-barrier interface (r_d=200 Å). It is clear that in both instances the "binding" energy E of the electron increases, as expected, with the increased Coulombic attraction resulting from the larger values of Λ. However, there is a marked difference in the magnitude of the effect between the two donor positions.

A decrease in the permittivity of the material in the vicinity of the donor implies a localized increase in the Coulombic attraction of the electron to the donor. Allowing for the self-consistent adjustment of the electron wave function, it turns out that when the donor is located at the center of the well this also coincides with the maximum in the probability distribution of the electron. Consequently the central cell correction can lead to a large increase in the binding energy of the electron. The latter is accompanied by a substantial reduction in the Bohr radius λ, as shown in Fig. 3, which in turn leads to a significant change of the electron wave function Ψ as depicted in Fig. 4. Conversely, when the donor is located at the well-barrier interface, the localized increase

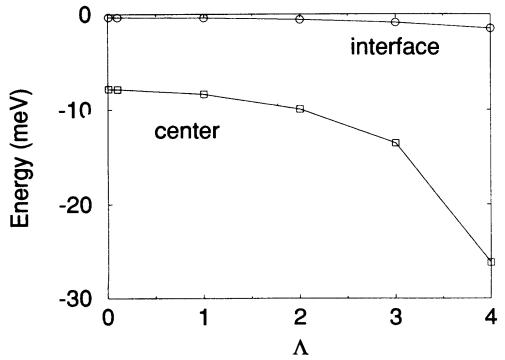

FIG. 2. Effect of the central cell correction parameter Λ (given in angstroms) on the energy of an electron in a donor–quantum-well system, for donors located either at the center or the interface of the well.

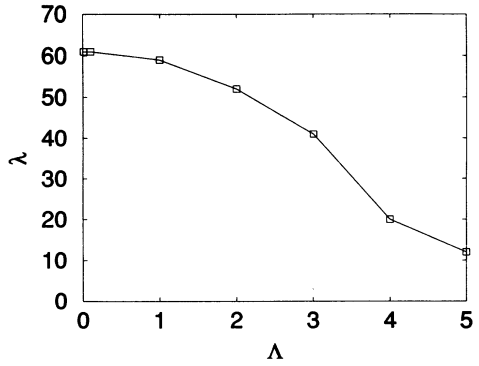

FIG. 3. Effect of the central cell correction parameter Λ on the Bohr radius of the electron-donor system, with the donor situated at the center of a 100 Å CdTe quantum well surrounded by barriers of $Cd_{0.925}Mn_{0.075}Te$ barriers.

in the Coulombic attraction occurs in a region which is spatially separated (~50 Å) from the peak in the electron probability distribution and hence the effect of the central cell correction is reduced correspondingly. This is the reason why the energy curve for this case shown in Fig. 2 is relatively independent of the parameter Λ. For this same situation, the Bohr radius λ is also virtually independent of Λ.

The actual extent of the central cell correction, as represented by the parameter Λ, can only be deduced by a careful comparison of experiment with theory. Figures 2 and 3 illustrate a possible approach for deducing Λ, namely, by measuring spectroscopically the energy of the donor-bound exciton emission from quantum wells which contain donors that are δ doped either at the center of the well or at the well-barrier interface. Comparison with the free exciton emission, and a knowledge of the binding energy of an exciton to a donor,[13] would enable a deduction of the magnitude of the central cell correction to be made, i.e., an evaluation of the parameter Λ.

C. Spin-flip Raman spectroscopy of double quantum wells

As mentioned earlier, one of the advantages of the present approach is its applicability to any form of potential $\mathcal{V}(z)$ occurring in semiconductor heterostructures.

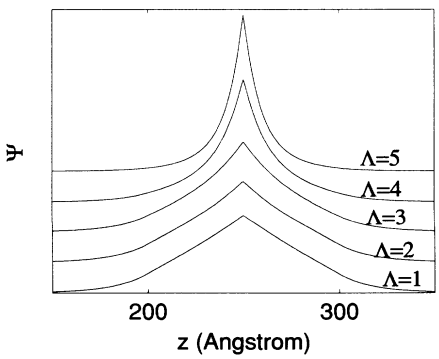

FIG. 4. Effect of Λ on the wave function Ψ of the electron bound to a donor corresponding to Fig. 3.

To illustrate the technique, we will calculate the energies associated with the Raman shifts due to spin flips of electrons attached to donors in a double quantum well structure. In the present section the central cell correction is omitted in the interests of clarity.

The double quantum well structure is shown schematically in Fig. 5. It consists of a 200 Å $Cd_{0.89}Mn_{0.11}Te$ outer barrier, a 100 Å $Cd_{0.97}Mn_{0.03}Te$ magnetic well, followed by a 20 Å $Cd_{0.89}Mn_{0.11}Te$ central barrier, a narrow 50 Å CdTe well, and finally a 200 Å outer barrier of $Cd_{0.89}Mn_{0.11}Te$. In a magnetic field the degeneracy of the electron (and hole) spin states in the semimagnetic $Cd_{1-x}Mn_xTe$ is lifted,[14] with the $m_J=+1/2$ state band edge increasing by $3A$ and the $m_J=-1/2$ band edge decreasing by $3A$. Gaj *et al.*[15] demonstrated that this giant Zeeman splitting could be expressed in the form of a modified Brillouin function B_J, i.e.,

$$A=-\frac{1}{6}xN_0\alpha s_0(x)B_J[\mathbf{B},x,T,T_0(x)], \tag{27}$$

where $s_0(x)$ and $T_0(x)$ are x dependent parameters,[15] the effective spin $s_0(x)$ accounts for the antiferromagnetic spin pairing of neighboring Mn^{2+} ions, and $N_0\alpha$=220 meV for $Cd_{1-x}Mn_xTe$.

Figure 6 shows the energy of an electron in the donor–double-quantum-well structure, for both spin states, in the presence of an external magnetic field of 6 T, as a function of donor position. It can be seen that the curve corresponding to the $+1/2$ spin component of the electron contains just one minimum, whereas the $-1/2$ spin component contains two minima. A plot of the wave function for the $-1/2$ spin state, across the whole structure for various positions of the donor ranging from r_d=0 to r_d=550 Å, is shown in Fig. 7. From the latter it can be seen that the energy minimum centered on 250 Å is attritutable to localization of the electron in the wide (magnetic) well, whereas the energy minimum centered on 340 Å is due to localization of the electron in the narrow well.

Spin-flip Raman spectroscopy exploits the Zeeman splitting of the conduction band and permits measurement of the energy difference E_{SF} between the two spin states of the conduction band electrons. Figure 8 shows the energy E_{SF}, corresponding to an electron spin flip between the two spin components of Fig. 6, as a function of donor position. If the donors are assumed to be uniformly distributed across the entire heterostructure it is possible, as demonstrated in Fig. 9, to represent the data of Fig. 8 in the form of an intensity I versus spin-

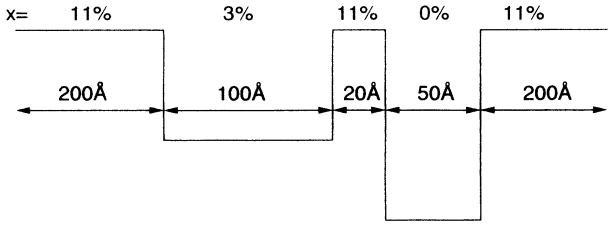

FIG. 5. Schematic representation of the double quantum well structure.

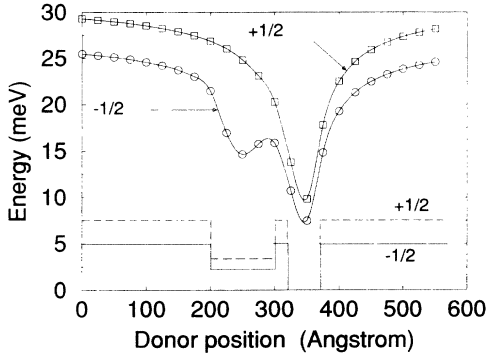

FIG. 6. Energy E of an electron in a donor–double-quantum-well system in a magnetic field of 6 T, for both electron spin states, as a function of the donor position r_d, together with a schematic illustration of the corresponding conduction band potential.

flip energy E Raman spectra, by assigning a Gaussian distribution to each point in energy space with a certain linewidth, i.e.,

$$I=\sum_{r_d}\frac{1}{\sigma\sqrt{2\pi}}\exp-\frac{[E-E_{SF}(r_d)]^2}{2\sigma^2}, \tag{28}$$

where $E_{SF}(r_d)$ is the spin-flip energy of the donor at position r_d and the standard deviation σ is related to the linewidth l (full width at half maxima) by

$$\sigma=\frac{l}{2\sqrt{2\ln 2}}. \tag{29}$$

Figure 9 shows the effect of different linewidths on the predicted Raman spectra of the double quantum well. In the lowest curve ($l=1$ cm^{-1}) it is possible in principle to resolve the donors in the left-hand barrier from those in the right-hand barrier. However, although this resolution is lost with increasing linewidth $l=1\longrightarrow 4$ cm^{-1}, the high energy peak (~82 cm^{-1}) corresponding to a spin flip in the wide magnetic well is still clearly distinguishable. Also, even though the low energy peak (~18 cm^{-1}) becomes a shoulder to the spin-flip energy of donors in

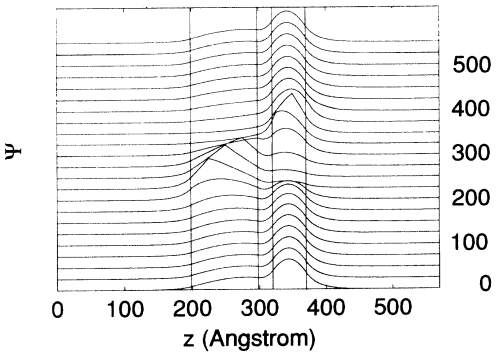

FIG. 7. Wave function Ψ for electron spin state $-1/2$, as a function of donor position, from r_d=0 (bottom) to r_d=550 Å (top).

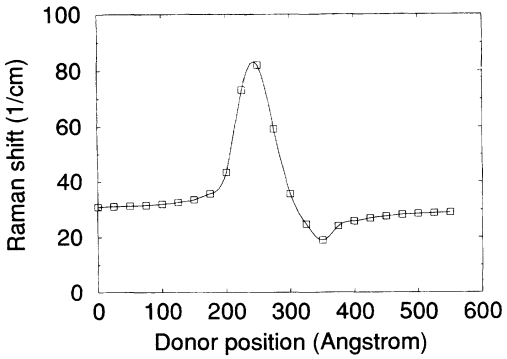

FIG. 8. Raman shift at 6 T as a function of donor position for the double quantum well of Fig. 5.

the barriers, it is still visible at l=4 cm^{-1}.

In conclusion we have demonstrated the important role of theoretical modelling for the interpretation of Raman spectra from double quantum well systems. In particular the method employed here allows the spin flips observed to be clearly identified and offers insight into the electron localization processes responsible for the spin-flip spectra.

D. δ doping as a probe of interface effects

It has been proposed that the magnetic behavior of the first few monolayers of a dilute magnetic semiconductor adjacent to an interface with a nonmagnetic semiconductor could be significantly different from that of the bulk.[16–18] One contribution to this effect arises from a reduction in the number of antiferromagnetically coupled pairs due to a decrease in the number of nearest neighbor magnetic ions.[16] A single layer of donors δ doped into a quantum well structure in the region of the well-barrier interface could provide a useful probe of the magnetism—via observation of spin-flip Raman spectroscopy.

As shown above, the effect of the central cell correction on the electron energy is negligible when the donor is located at the well-barrier interface of a relatively wide (100 Å) well. In the present section a narrower well (40 Å) with lower potential barriers ($Cd_{0.98}Mn_{0.02}Te$) is chosen so as to enhance any interface effects—the electron probability density at the interface of a narrower well being higher than in a wide well. However, the central cell correction is still neglected for the reasons mentioned above, namely, its effects are anticipated to be small and its inclusion would not affect the essential points being made.

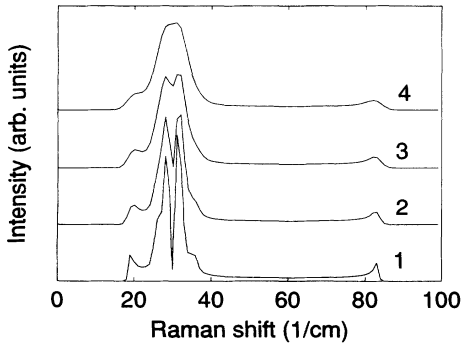

FIG. 9. Simulated spin-flip Raman spectra for assumed linewidths l of 1 cm^{-1} (bottom) to 4 cm^{-1} (top).

Assuming the exchange integral $N_0\alpha$ associated with a dilute magnetic semiconductor does not change near an interface with a nonmagnetic material, then a decreasing number of nearest neighbors for each magnetic ion would imply an increased paramagnetism. Now the product $xs_0(x)$ in Eq. (27) can also be written as $x_{\rm eff}s$, where s is the spin of a magnetic ion, in this case $s = 5/2$. This allows the magnetism to be discussed in terms of an effective manganese concentration $x_{\rm eff}$. In the present series of calculations the effective concentration near an interface was expressed in the form

$$x_{\rm eff}^{\rm int} = \zeta x_{\rm eff}, \tag{30}$$

i.e., if ζ=1, there is no enhancement of the magnetism, but $\zeta > 1$ corresponds to enhancements of the magnetism. Independent work[12] has suggested that the enhanced magnetism extends over about two monolayers adjacent to the interface. Figure 10 shows the effect on the potential of this enhanced magnetism, for the +1/2 spin state corresponding to a value of ζ=4 over a two monolayer region. The corresponding electron wave function Ψ associated with a donor located at the well-barrier interface, i.e., r_d=340 Å in each of these potentials, is also shown in Fig. 10. Although there appear to be only minor differences in the two wave functions, the effect of the increased interface magnetism on the energy of an electron in the donor–quantum-well system is marked. This is shown in Fig. 11 where the corresponding spin-flip Raman shift at a field high enough to saturate the Mn^{2+} ions is shown as a function of the parameter ζ. The figure shows that such enhancements in the magnetism would lead to appreciable changes in the Raman shifts of donors at the magnetic-nonmagnetic interface. It is clear from these considerations that experiments involving the δ doping of donor atoms in quantum well structures at various positions in the well and barrier when coupled

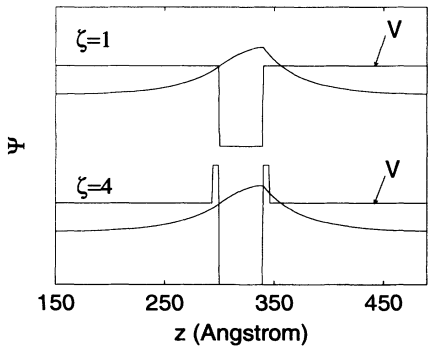

FIG. 10. Effect of enhanced paramagnetism at the magnetic-barrier–nonmagnetic-well interface (as represented by the parameter ζ) on the potential and the wave function Ψ of an electron bound to a donor situated at the well-barrier interface.

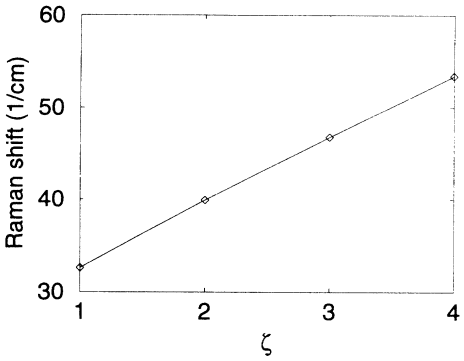

FIG. 11. Effect of enhanced paramagnetism on the spin-flip Raman shift for donors located at the well-barrier interface.

with calculations of the type presented here should permit a determination of any enhancements in the magnetism at heterojunctions, via the use of spin-flip Raman spectroscopy.

IV. CONCLUSION

An approach for calculating binding energies of neutral donors in semiconductor heterostructures has been presented and its extension to include effects such as band nonparabolicity, effective mass mismatch at heterojunctions, and central cell corrections described. The utility of such calculations have been demonstrated by evaluating the spin-flip Raman spectrum of double quantum wells. Furthermore it has been demonstrated that spin-flip Raman spectroscopy, together with δ doping of donor atoms, would be an ideal probe of the effects of interfaces on the magnetic properties of dilute magnetic semiconductors.

APPENDIX

Consider the term

$$\nabla_x e^{-\frac{r'}{\lambda}} = \frac{\partial}{\partial r'} e^{-\frac{r'}{\lambda}} \frac{\partial r'}{\partial x} = -\frac{x}{r'\lambda} e^{-\frac{r'}{\lambda}} \tag{A1}$$

and similarly

$$\nabla_x^2 e^{-\frac{r'}{\lambda}} = \left(-\frac{1}{r'\lambda} + \frac{x^2}{\lambda r'^3} + \frac{x^2}{r'^2\lambda^2} \right) e^{-\frac{r'}{\lambda}}. \tag{A2}$$

Similar expressions follow for the y and z directions to give

$$\nabla^2 e^{-\frac{r'}{\lambda}} = \left(-\frac{2}{r'\lambda} + \frac{1}{\lambda^2} \right) e^{-\frac{r'}{\lambda}}. \tag{A3}$$

[1] C. Mailhiot, Yia-Chung Chang, and T. C. McGill, Phys. Rev. B **26**, 4449 (1982).
[2] R. L. Greene and K. K. Bajaj, Solid State Commun. **45**, 825 (1983).
[3] S. Chaudhuri and K. K. Bajaj, Phys. Rev. B **29**, 1803 (1984).
[4] Chong-ru Huo, Ben-Yuan Gu, and Lei Gu, J. Appl. Phys. **70**, 4357 (1991).
[5] P. Harrison, T. Stirner, and W. E. Hagston, Phys. Rev. B **47**, 16 404 (1993).
[6] G. A. Bastard, *Wave Mechanics Applied to Semiconductor Heterostructures* (Les Editions de Physique, Paris, 1988).
[7] P. Harrison, J. P. Goodwin, and W. E. Hagston, Phys. Rev. B **46**, 12 377 (1992).
[8] W. H. Press, B. P. Flannery, S. A. Teukolsky, and W. T. Vetterling, *Numerical Recipes* (Cambridge University Press, Cambridge, 1986).
[9] J. P. Killingbeck, *Microcomputer Algorithms* (Hilger, Bristol, 1992).
[10] S. Fraizzoli, F. Bassani, and R. Buczko, Phys. Rev. B **41**, 5096 (1990).
[11] U. Ekenberg, Phys. Rev. B **40**, 7714 (1989).
[12] S. Jackson, J. E. Nicholls, W. E. Hagston, P. Harrison, T. Stirner, and J. H. C. Hogg (unpublished).
[13] S. Weston, T. Stirner, P. Harrison, J. E. Nicholls, W. E. Hagston, and D. E. Ashenford, J. Phys. (Paris) **3**, 397 (1993).
[14] *Semiconductors and Semimetals*, edited by J. K. Furdyna and J. Kossut (Academic, Boston, 1988), Vol. 25.
[15] J. A. Gaj, R. Planel, and G. Fishman, Solid State Commun. **29**, 435 (1979).
[16] D. R. Yakovlev, *Festkörperprobleme (Advances in Solid State Physics)* (Vieweg, Braunschweig, 1992), Vol. 32, p. 251.
[17] W. E. Hagston, P. Harrison, J. H. C. Hogg, S. R. Jackson, J. E. Nicholls, T. Stirner, B. Lunn, and D. E. Ashenford, J. Vac. Sci. Technol. B **11**, 881 (1993).
[18] T. Stirner, P. Harrison, W. E. Hagston, and J. P. Goodwin, J. Appl. Phys. **73**, 5081 (1993).